This article has been accepted for publication in Journal of Lightwave Technology (Volume:33, Issue: 4) Citation information: DOI 10.1109/JLT.2014.2373051

Connecting Silicon Photonic Circuits to Multi-Core Fibers by Photonic Wire Bonding

Nicole Lindenmann, Stephan Dottermusch, Maria Laura Goedecke, Tobias Hoose, Muhammad Rodlin Billah, Temitope Onanuga, Andreas Hofmann, Wolfgang Freude, *Senior Member, IEEE, Member OSA*, Christian Koos, *Member, IEEE, Member OSA*

(Invited Paper)

***Abstract*— Photonic wire bonding is demonstrated to enable highly efficient coupling between multi-core fibers and planar silicon photonic circuits. The technique relies on *in-situ* fabrication of three-dimensional interconnect waveguides between the fiber facet and tapered silicon-on-insulator waveguides. Photonic wire bonding can easily compensate inaccuracies of core placement in the fiber cross-section, does not require active alignment, and is well suited for automated fabrication. We report on the design, on fabrication, and on characterization of photonic wire bonds. In a proof-of-principle experiment, a four-core fiber is coupled to a silicon photonic chip, leading to measured coupling losses as small as 1.7 dB.**

***Index Terms* —[1]Integrated optics, nanotechnology, optical fibers, optical interconnections, waveguides, photonic wire bonding, two-photon lithography, silicon photonics, multi-core fibers**

INTRODUCTION

Over the last years multi-core fibers (MCF) have proven to dramatically increase the transmission capacity of optical links by enabling space-division multiplexing (SDM) [1]. For exploiting the full potential of SDM in real-world transmission systems, MCF need to be connected to highly integrated photonic transmitter and receiver circuitry. The associated fiber-chip interfaces still represent a major challenge: Unlike the cores of the MCF, waveguides in photonic integrated circuits (PIC) are arranged in a common plane, and edge coupling is hence impossible. To overcome this problem, out-of-plane connection of a seven-core fiber to a silicon-on-insulator PIC has been demonstrated using an array of grating couplers [2]. This technique requires elaborate active alignment for adjusting the relative position of the MCF and the PIC in six degrees of freedom and is therefore not well suited for industrial mass production. Moreover, because of random deviations of the core positions within the cross section of the MCF, it is impossible to optimize the coupling efficiencies of all core-chip interfaces simultaneously. For this reason, a rather high insertion loss of 9.8 dB was measured [2]. In addition, out-of-plane coupling impedes the construction of flat packages, where fiber axis and chip surface are aligned. Furthermore, transmission bandwidth of grating coupler connections is intrinsically limited, making the concept unsuited for massively parallel wavelength division multiplexing schemes that use a large number of channels.

In this paper we show that photonic wire bonding [3]-[4] provides a viable method for MCF-chip interfaces that overcome the limitations of grating couplers. Photonic wire bonding allows fabricating free-standing polymer waveguides with diameters down to 1 µm *in situ* by direct-write three-dimensional (3D) laser lithography based on two-photon polymerization. In previous experiments, we successfully

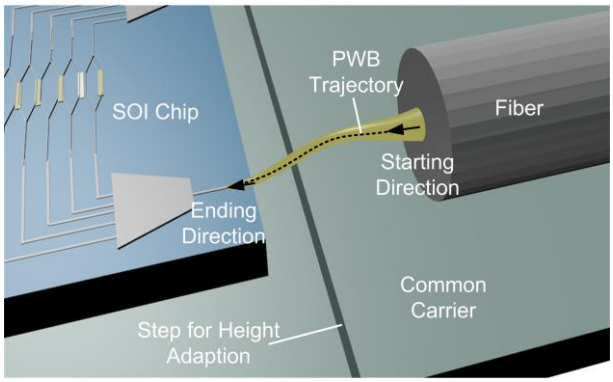

Fig. 1: Schematic of a photonic wire bond (PWB) between fiber and silicon-on-insulator (SOI) chip. The PWB trajectory is selected such that it adapts to the positions and the optical axes of the structures to be connected. Obstacles like chip or fiber edges must be avoided, and a good compromise is to be found between long interconnects and sharp waveguide bends.

This work was supported by the BMBF project PHOIBOS (grant 13N12574), by the EU-FP7 project BigPipes, by the European Research Council (ERC Starting Grant 'EnTeraPIC', grant 280145), by the Center for Functional Nanostructures (CFN) of the DFG (project A 4.7), by the Helmholtz International Research School for Teratronics (HIRST), by the Alfried Krupp von Bohlen und Halbach Foundation, by the Karlsruhe Nano-Micro Facility (KNMF), and by the Karlsruhe School of Optics and Photonics (KSOP).

Nicole Lindenmann, Stephan Dottermusch, Maria Laura Goedecke, Tobias Hoose, Muhammad Rodlin Billah, Temitope Onanuga, Wolfgang Freude and Christian Koos are currently with Karlsruhe Institute of Technology (KIT), Germany, Institute of Photonics and Quantum Electronics (IPQ) and Institute of Microstructure Technology (IMT) (e-mail: Nicole.Lindenmann@kit.edu, Christian.Koos@kit.edu). Andreas Hofmann is with Karlsruhe Institute of Technology, Institute of Applied Computer Science.

demonstrated single-mode interconnects of silicon PIC on different chips, showed transmission at terabit/s data rates, and reported ways to reduce the transmission loss of photonic wire bonds (PWB) interconnecting silicon-on-insulator (SOI) waveguides (WG) to 1.6 dB. Here we expand on these results and show coupling of a four-core fiber to a silicon photonic chip with insertion losses down to 1.7 dB. The technique renders active alignment obsolete, can easily compensate tolerances of the core placement, and lends itself to automated mass production. Moreover, the fiber can be positioned in the same plane as the chip surface, thereby enabling greatly simplified and fully planar packages.

I. Designing the Photonic Wire Bond

Besides being single-moded at a wavelength of 1550 nm, photonic wire bonds have to fulfill a number of other requirements: Most important are small losses over a large bandwidth, a physically feasible trajectory without intersecting obstacles, and a mechanically stable shape that withstands the capillary forces during the removal of the unexposed part of the resist, from which the PWB is made of. Fig. 1 shows a schematic illustration of a photonic wire bond interconnecting one core of a MCF and a SOI chip. In this example, the photonic wire bond has tapered sections on the fiber endface as well as towards the SOI chip for adapting the mode fields. Between the tapered structures, the PWB has a round cross-section, and the PWB axis follows a 3D trajectory in space. The following section describes the optimization of the PWB trajectory, and the design of the tapers near the MCF as well as near the nanophotonic SOI waveguides.

A. *Low-loss trajectory*

For minimum optical loss, the trajectory of a PWB axis has to obey a number of constraints. To begin with, the endfaces of the PWB must overlap with the connecting waveguides on both sides. Next, the starting and ending orientation of the PWB axes have to coincide with the connecting waveguide axes. Further, the trajectory of the PWB axis is to be chosen such that intersections with obstacles like fibers, chip edges or other PWB are avoided. Finally, increased losses by a strong curvature of the trajectory and a large length should be avoided, and a suitable compromise has to be found.

To fulfill the requirements listed above, a complicated optimization process has to be employed. Because the target (objective, cost) function is the optical transmission loss which has to be minimized, an appropriate loss model is needed for the PWB. While the theory of waveguide bends lying in a plane is well developed [5]-[8], no theory is available for a waveguide with an axis which is bent in three dimensions. Work is in progress to find the parameters of a closed-form empirical function for the PWB losses. Meanwhile, with the help of full-wave finite-integration technique (FIT) calculations (CST Microwave Studio), we developed an expert system for designing the trajectories empirically, based on fifth-order polynomials.

B. *Fiber interface*

The fiber interface serves to convert the MCF mode field to the fundamental mode of the PWB. This interface is realized by a linear up-taper of the PWB waveguide; see Fig. 2. For

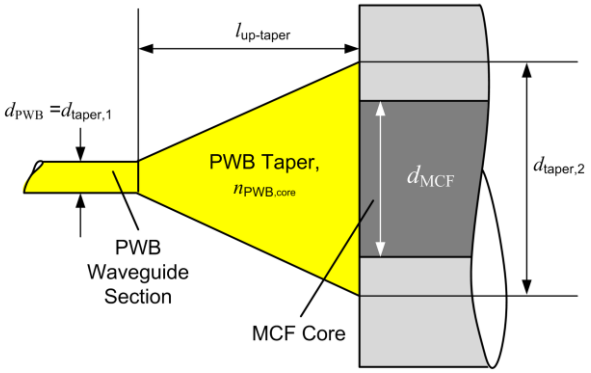

Fig. 2: Structure of the linear up-taper used at the interface between the MCF and the PWB. The taper starts with the circular cross-section of the PWB (d_{PWB} = $d_{taper,1}$ = 2 µm) and ends with a circular cross section of larger diameter $d_{taper,2}$ at the fiber endface. This taper ending diameter is optimized for minimum insertion loss and turns out to be larger than the fiber core diameter d_{MCF} = 8 µm, because the relative refractive index difference between core and cladding is much larger for the PBW ($n_{PWB,core}$ = 1.53 $n_{PWB,clad}$ = 1.34, Δ_{PWB} = 13 % at 1550 nm) than for the fiber (Δ_{MCF} = 0.54 % at 1550 nm).

designing the taper, we perform FIT simulations. We use a four-core fiber provided by Fibercore Inc. (SM-4C1500), featuring a step-index profile with a relative refractive index difference between core and cladding of Δ_{MCF} = 0.54 % [9], a core diameter of d_{MCF} = 8 µm, and a (Gaussian) mode-field diameter of 8.4 µm (1/e-diameter of the modal amplitude) as specified by the manufacturer. The PWB consists of a commercially available polymer with a refractive index of $n_{PWB,core}$ = 1.53 at a wavelength of 1550 nm (IP-Dip™, [10]). The diameter of the circular PWB cross-section is d_{PWB} = 2 µm. The PWB is embedded in a low-index material that acts as an optical cladding as well as a mechanical support. We prefer *Cytop*™ [11] as a cladding material, having a refractive index of $n_{PWB,clad}$ = 1.34. The relative refractive index difference $\Delta = \left(n_1^2 - n_2^2\right)/\left(2n_1^2\right)$ between PWB core and

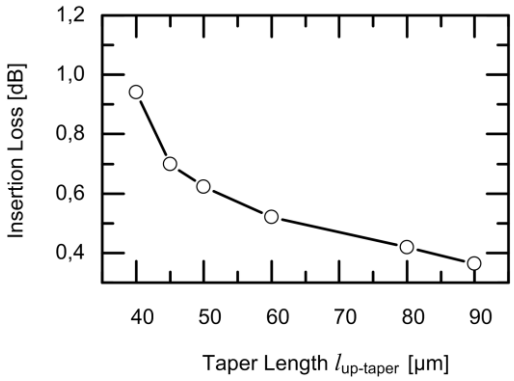

Fig. 3: Calculated insertion loss for optimized interfaces between the MCF and the PWB. A linear polymer taper with circular cross-section is used between the endface of the MCF (core diameter d_{MCF} = 8 µm, Δ_{MCF} = 0.54 % at 1550 nm) and the single-mode PWB section (core diameter d_{PWB} = 2 µm, core index $n_{PWB,core}$ = 1.53, cladding index $n_{PWB,clad}$ = 1.34 at 1550 nm). The diameter of the taper at the MCF interface is optimized for mimimum insertion loss. The insertion loss is calculated between the fundamental eigenmode of the MCF and the fundamental eigenmode of the PWB waveguide section.

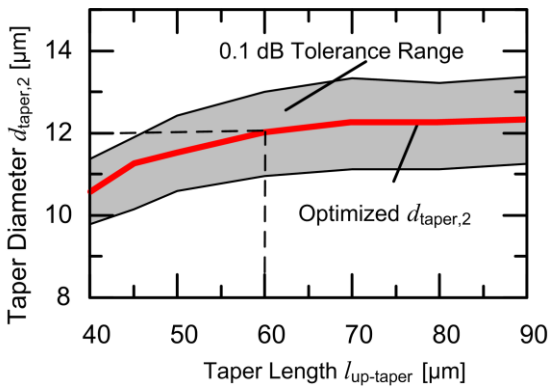

Fig. 4: Taper diameter $d_{taper,2}$ at the MCF interface vs. taper length $l_{up\text{-}taper}$ for a loss-optimized structure (red line). The linear polymer taper connects the single-mode PWB section (diameter d_{PWB} = 2 µm) with the endface of the MCF (SM-4C1500 core diameter d_{MCF} = 8 µm). At a taper length of 60 µm, the optimum taper diameter at the MCF interface amounts to $d_{taper,2}$ = 12 µm, and the minimum achievable transmission loss is 0.52 dB. In this case, the taper diameter $d_{taper,2}$ may vary between 10.9 µm and 13.0 µm for an increase of the insertion loss by at most 0.1 dB.

cladding is Δ_{PWB} = 13 %, indicating a strong guidance.

Parameter sweeps of taper length and taper diameter at the fiber endface result in a loss-optimized taper diameter as a function of the taper length, see Fig. 3. The shaded area in Fig. 4 shows the region where the minimum insertion loss (red line) increases by 0.1 dB. For a taper length of $l_{up\text{-}taper}$ = 60 µm, a taper diameter range between 10.9 µm and 13.0 µm leads to a loss increase of less than 0.1 dB. This shows that the taper design is stable with respect to production tolerances and therefore well suited for fabrication. The simulated insertion loss of optimized tapers as a function of length is depicted in Fig. 3. The calculated loss between PWB and MCF amounts to 0.52 dB at a taper length of $l_{up\text{-}taper}$ = 60 µm and taper diameter of 12 µm.

C. SOI chip interface

Next, we need to connect the PWB to a silicon-on-insulator strip waveguide that consists of a nanophotonic waveguide core on top of a thick buried oxide layer. An illustration of the interconnect is depicted in Fig. 5. For a low-loss transition between PWB and SOI WG we have to increase the mode field diameter of the SOI WG. This is done by laterally down-tapering the SOI WG towards the PWB ("inverse taper") [12], and by embedding the SOI WG into a rectangular polymer waveguide that is down-tapered towards the SOI WG. We refer to this structure as a 3D double-taper in the following. The 3D double-taper is covered by a cladding material. Fig. 5 shows the double-taper structure. The SOI WG tip has a width of w_{tip} = 80 nm. Measured from this tip, the investigated SOI WG taper lengths lie between l_{Si} = 40 µm and l_{Si} = 100 µm. The SOI WG taper connects to a straight SOI WG with a cross-section of w_{Si} = 500 nm (width) by h_{Si} = 220 nm (height). The PWB taper has a cross-section of $w_{PWB,taper,1}$ = 0.76 µm by $h_{PWB,taper,1}$ = 0.45 µm and ends with a cross-section of $w_{PWB,taper,2}$ = 2 µm by $h_{PWB,taper,2}$ = 2 µm at the PWB waveguide side. The length of the polymer taper is fixed to $L_{PWB,taper}$ = 80 µm.

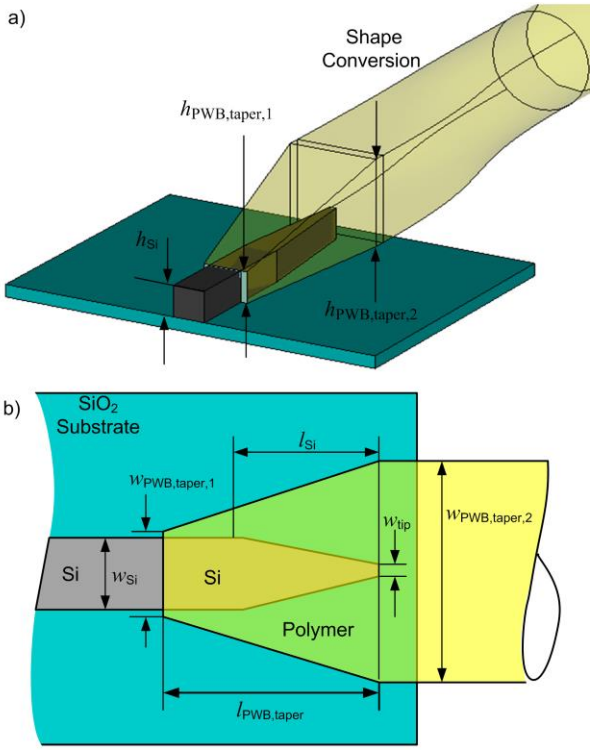

Fig. 5: 3D double-taper structure for modal field match between PWB and SOI waveguide. (a) The SOI WG ends in a laterally down-tapered section ("inverse taper"), whereas the PWB features a section that is laterally and vertically down-tapered to adiabatically transform the SOI waveguide mode to that of the PWB. The PWB waveguide section gradually changes its cross-section from rectangular to circular. (b) The SOI WG tip has a width of w_{tip} = 80 nm. The SOI WG taper connects to a straight SOI WG with a cross-section of w_{Si} = 500 nm by h_{Si} = 220 nm. Measured from this tip, the investigated SOI WG taper lengths lie between l_{Si} = 40 µm and l_{Si} = 100 µm. The PWB taper has a rectangular cross-section of $w_{PWB,taper,1}$ = 0.76 µm by $h_{PWB,taper,1}$ = 0.45 µm and ends with a rectangular cross-section of $w_{PWB,taper,2}$ = 2 µm by $h_{PWB,taper,2}$ = 2 µm at the PWB waveguide section. The length of the PWB taper is fixed to $L_{PWB,taper}$ = 80 µm. The lower-index cladding material is not displayed here for the sake of clarity.

The rectangular PWB gradually changes its shape to a cylindrical PWB over a length of 20 µm. Polymer taper and PWB consist of the same material and are fabricated simultaneously.

The loss of the 3D double-taper is calculated between the fundamental eigenmode of the clad *rectangular* polymer taper WG and the fundamental eigenmode of the straight SOI WG. Again we employ a FIT solver, and we use the following additional data, all valid at a wavelength of 1550 nm: Refractive indices of silicon (n_{Si} = 3.48), silicon dioxide (n_{SiO2} = 1.44), PWB taper ($n_{PWB,core}$ = 1.53), and cladding ($n_{PWB,clad}$ = 1.34). The silicon taper length varies between l_{Si} = 40 µm and l_{Si} = 100 µm. Except for the l_{Si} = 40 µm and l_{Si} = 100µm long SOI WG taper, the calculated losses lie between 0.75 dB and 0.9 dB in the C-Band (1530 nm - 1565 nm), see Fig. 6. Obviously, the 40 µm taper is too short for a low-loss transition. We attribute the ripple in the loss curves to multiple internal reflections inside the 3D double-taper.

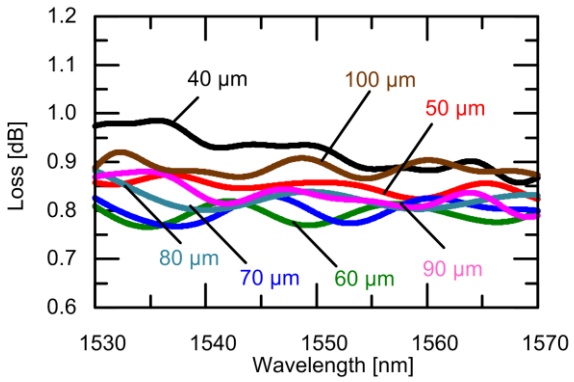

Fig. 6: Simulated transmission over wavelength for a 3D double-taper interface as shown in Fig. 5. The following values apply for the SOI waveguide: w_{Si} = 500 nm, h_{Si} = 220 nm, taper tip width w_{tip} = 80 nm, refractive index n_{Si} = 3.48 at 1550 nm. For the PWB taper: initial height $h_{PWB,taper,1}$ = 450 nm, initial width $w_{PWB,taper,1}$ = 760 nm, PWB waveguide section $w_{PWB,taper,2}$ = 2 µm × $h_{PWB,taper,2}$ = 2 µm, $n_{PWB,core}$ = 1.53 and $n_{PWB,clad}$ = 1.34 both at 1550 nm. The silicon taper length l_{Si} is varied in the simulation between l_{Si} = 40 µm and l_{Si} = 100 µm. Except of the l_{Si} = 40 µm and l_{Si} = 100 µm long SOI taper the simulation losses range between 0.75 dB and 0.9 dB.

II. Fabrication

For the realization of the photonic wire bond several fabrication steps are required. First, the objects to be interconnected (MCF and SOI WG in our example) are mounted on a common carrier using standard pick-and-place machinery with moderate precision. In this experiment we used a glass carrier with two different height levels for rough adjustment of the component heights, and we fixed the components with glue.

Second, the interconnect regions (MCF endface and SOI WG end) are embedded into a negative-tone photoresist, and the actual positions of the optical connection points (fiber core endfaces and taper tips of SOI WG) are detected by microscope image processing. With these data, the PWB shape (trajectory and waveguide cross-section along the trajectory) is calculated according to the criteria described previously.

Third, the calculated waveguide structures are defined by a direct-write 3D lithography technique. In our experiment, we use a commercial lithography system (*Photonic Professional* from *Nanoscribe GmbH*) [10], which uses a frequency-doubled fiber laser emitting pulses at 780 nm wavelength with approximately 80 MHz repetition frequency and <100 fs pulse width. This laser light is focused into the resist through an immersion objective (100× magnification) with a large numerical aperture (NA = 1.3). The power at the input pupil of the objective amounts to approximately 4 mW. We use a high-resolution photo-resist (IP-Dip™), which is transparent at the laser wavelength, but enables two-photon polymerization in the high-intensity focal spot of the lithography system. Depending on the NA of the objective, on the laser power and on the sensitivity of the photo-resist, such a volume element (voxel) has a diameter (height) down to 100 nm (200 nm) [13]. In the lithography step, a refined two-stage writing strategy is used to define the PWB structures by moving the focal spot of the writing beam through the volume of the resist, see Fig. 7. The inner volume is exposed first by writing spiral lines, and an outer shell of contour lines is then added to smoothen the surface.

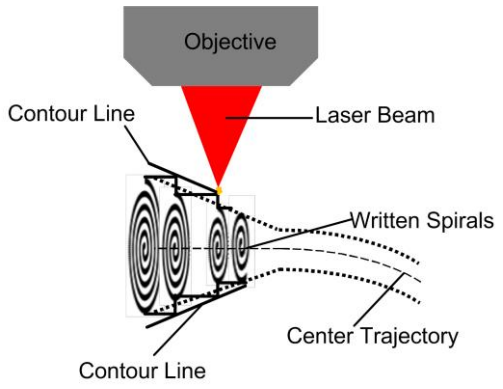

Fig. 7: Two-step writing strategy for PWB fabrication. The inner volume is exposed first by writing spiral lines. In a second step, an outer shell is added by writing lines parallel to the contour of the PWB for smoothening the surface.

As a last fabrication step, the unexposed resist material is removed in a developer bath, and the resulting PWB is finally embedded in a low-index cladding material. In our experiments we immerse the photonic wire bond into an index-matching liquid with a refractive index of 1.34, but a low-index cladding material like *Cytop*™ would be preferred for stabilization.

For practical application of photonic wire bonding in manufacturing, writing speed is a crucial parameter. We are currently using a system, in which the lateral movement of the lithography beam is steered with galvanometer-driven scanning mirrors. For this system, achievable writing times amount to less than 5 min for a fiber-chip PWB. This is much faster than our conventional system, in which the focus of the laser beam was held in a fixed position and the high-inertia sample holder had to be moved by a piezo-driven translation stage, leading to writing speeds of approximately 75 µm/s and writing times of more than 1h per fiber-chip PWB. The structures presented below have still been written using the piezo system. For scanner-based lithography systems, we expect that further

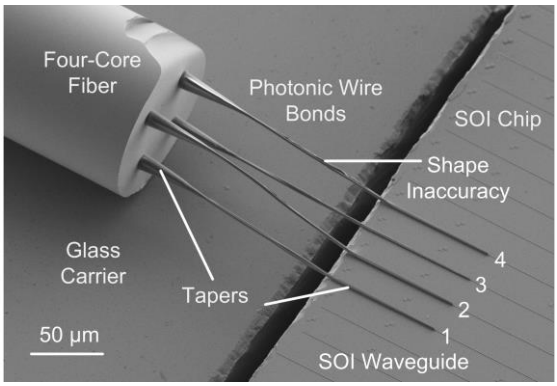

Fig. 8: Fabricated sample. Photonic wire bonds (PWB) connect the individual cores of a four-core fiber to different on-chip SOI waveguides. The PWB are up-tapered both on the MCF and on the SOI WG side to match the mode diameter to that of the fiber core and of the SOI WG, respectively. The PWB consist of a negative-tone photo-resist. At PWB 4, shape imperfections can be seen.

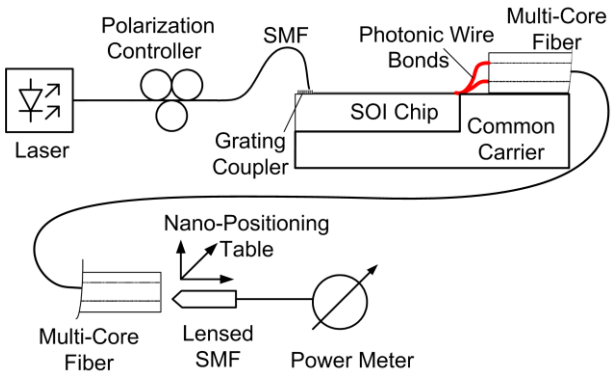

Fig. 9: Measurement setup. Laser light is coupled to the individual SOI waveguides by grating couplers, and then passed on to the MCF via the PWB connection. The cleaved output facet of the MCF is scanned by a lensed fiber to measure the power distributions.

optimization will allow writing times of a few seconds per fiber-chip PWB in the future, making the technique suited for high-volume mass production.

III. Multi-Core Fiber-Chip Connection

Fig. 8 shows the resulting PWB interconnection between a four-core fiber and a silicon photonic chip. The interface consists of four PWB that connect the individual cores of the MCF to different on-chip waveguides.

At the interface towards the SOI WG, polymer tapers of length $L_{PWB,taper}$ = 80 µm are used. Their initial cross-sections are rectangular with $w_{PWB,taper,1}$ = 0.76 µm (width) and $h_{PWB,taper,1}$ = 0.45 (height), and they end with a quadratic cross-section of equal width and height, $w_{PWB,taper,2}$ = $h_{PWB,taper,2}$ = 2 µm at the PWB waveguide section. The embedded Si tapers have a length of l_{Si} = 60 µm and a taper tip width of w_{tip} = 80 nm as described in Section I C. The PWB tapers towards the fiber endface have a starting diameter of $d_{taper,2}$ = 12 µm and a taper length of $l_{up\text{-}taper}$ =60 µm The circular PWB waveguide sections have diameters of d_{PWB} =2 µm as described in Section I B.

For measuring the insertion losses of the MCF-chip interconnects, we use the setup depicted in Fig. 9. Light is coupled to the individual SOI waveguides via grating couplers, and then passed on to the MCF cores via the PWB interface. The cleaved output facet at the far end of the MCF is scanned by a lensed fiber to measure the power distribution in the cross-section as depicted in Fig. 10. The best performance is found if light is launched into waveguide number 2. In this case we measure a total loss of 9.7 dB for an optimum alignment of the lensed SMF. Taking into account insertion losses of 4.8 dB at the grating-coupler interface and another 3.2 dB of coupling loss between the MCF core and the lensed fiber, we find a net insertion loss of 1.7 dB for the PWB interface. The losses of the grating-coupler interface were determined from a reference measurement, revealing a loss of 9.6 dB when coupling light through a simple SOI WG with two grating couplers. Similarly, the insertion loss between the MCF core and the lensed fiber has been obtained from a reference transmission experiment comprising a pair of lensed fibers and a piece of MCF. Applying the same technique to the remaining bonds 1, 3, and 4, we find insertion losses of 3.5 dB, 2.5 dB, and 6.8 dB, respectively.

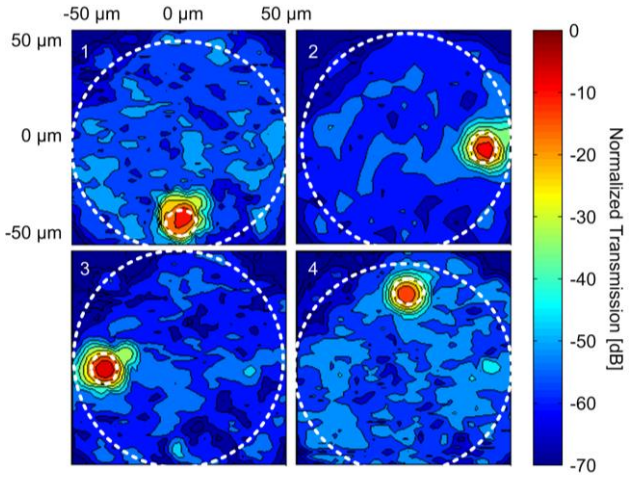

Fig. 10: Spatially resolved normalized power transmission at the cleaved output facet of the multi-core fiber. The transmission is normalized to the maximum power level in each core, measured when launching light to the individual on-chip waveguides 1…4. These data correspond to insertion losses of 3.5 dB (PWB 1), 1.7 dB (PWB 2), 2.5 dB (PWB 3) and 6.8 dB (PWB 4). The rather high insertion loss of PWB 4 is attributed to fabrication imperfections, see Fig. 8 The net insertion loss of the MCF-chip interface is obtained by taking into account the losses of the grating-coupler interface (4.8 dB) and the coupling losses between the MCF-core and lensed fiber (3.2 dB).

All measurements were performed under usual laboratory conditions without special temperature control. The performance of photonic wire bonds under more challenging environmental conditions such as high temperatures and higher humidity is subject to ongoing research. In first tests we found that PWB maintain performance after being baked at 85°C at normal atmosphere for one hour, and multiple rinses in water also did not worsen the transmission of PWB. We therefore expect the structures to exhibit stability properties that are well suited for a wide range of practical applications.

Simulated losses of the fabricated structure amount to 1.3 dB, where 0.78 dB are due to the transition between the PWB and the SOI WG, and the remaining 0.52 dB are caused by the interface to the MCF. This compares well to the smallest measured insertion loss of 1.7 dB – the additional losses are attributed to scattering losses in the PWB waveguide section itself, caused by fabrication imperfections which cannot be included in the simulations, see Fig. 8. Moreover, shrinkage of the resist after exposure led to tension within the PWB, see Fig. 8. We believe that transmission and uniformity of the MCF-chip interfaces can be significantly improved in the future by optimizing taper structures and fabrication processes, leading to insertion losses of less than 1 dB for a fiber-chip interface.

IV. Summary

We show that photonic wire bonding enables low-loss interfaces between multi-core fibers and single-mode SOI

waveguides. The technique does not require active alignment and allows connecting a wide range of fiber types and core configurations. Insertion losses as down to 1.7 dB were measured, with much potential for further improvement.

ACKNOWLEDGMENT

We acknowledge Fibercore Inc. for providing the multi-core fiber and Nanoscribe GmbH for fruitful discussion.

REFERENCES

[1] H. Takara *et al.*, "1.01-Pb/s (12 SDM/222 WDM/456 Gb/s) crosstalk-managed transmission with 91.4-b/s/Hz aggregate spectral efficiency," in *European Conf. and Exhibition on Optical Communication*, 2012, Paper Th.3.C.1.

[2] C. R. Doerr and T. F. Taunay, "Silicon photonics core-, wavelength-, and polarization-diversity receiver," *IEEE Photonics Technol. Lett*., vol. 23, no. 9, pp. 597–599, 2011.

[3] N. Lindenmann *et al.*, "Photonic wire bonding: a novel concept for chip-scale interconnects.," *Opt. Express*, vol. 20, no. 16, pp. 17667–17677, Jul. 2012.

[4] N. Lindenmann *et al.*,"Connecting silicon photonic circuits to multi-core fibers by photonic wire bonding," in l*EEE Optical Interconnects Conference*, Coronado (CA), USA, 2014, Paper WD1.

[5] M. Heiblum and J. Harris, "Analysis of curved optical waveguides by conformal transformation," *IEEE J. Quantum Electron*., vol. 11, no. 2, 1975.

[6] K. R. Hiremath, M. Hammer, R. Stoffer, L. Prkna, and J. Čtyroký, "Analytic approach to dielectric optical bent slab waveguides," *Opt. Quant. Electron.*, vol. 37, pp. 37–61, 2005.

[7] E. A. J. Marcatili, "Bends in optical dielectric guides," *Bell Syst. Tech. J*., vol. 48, no. 7, pp. 2103–2132, 1969.

[8] D. Marcuse, "Bending losses of the asymmetric slab waveguide," *Bell Syst. Tech. J*., vol. 50, no. 8, pp. 2551–2563, Oct. 1971.

[9] A. D. Yablon, "Multifocus tomographic algorithm for measuring optically thick specimens.," *Opt. Lett*., vol. 38, no. 21, pp. 4393–6, Nov. 2013.

[10] www.nanoscribe.de

[11] http://www.agcce.com/Cytop.asp

[12] V. R. Almeida, R. R. Panepucci, and M. Lipson, "Nanotaper for compact mode conversion.," *Opt. Lett*., vol. 28, pp. 1302–1304, 2003.

[13] H. Sun and S. Kawata, "Two-photon photopolymerization and 3D lithographic microfabrication," *Adv. Polym. Sci*., vol. 170, pp. 169–274, 2004.

Nicole Lindenmann received her diploma in Physics with a focus on Optical Communications at Karlsruhe Institute of Technology in 2009. Since 2010 she has been working as doctoral researcher at the Institute of Photonics and Quantum Electronics (IPQ) and the Institute of Microstructure Technology (IMT) where she developed photonic wire bonding as a novel approach in optical interconnect technologies. Her work also focuses on integrated optics in silicon and polymers as well as on the interfaces between different photonic platforms.

Stephan Dottermusch received his M.Sc. degree in Physics from Karlsruhe Institute of Technology (KIT) in 2014. His work focused on adapting the technique of photonic wire bonding for bridging between integrated silicon photonics and optical fibers. He is currently working towards his Ph.D. in the field of nanophotonics for solar energy.

Maria Laura Goedecke earned the B.Sc. degree in Physics at Ulm University in 2012. She is currently working towards the M.Sc. degree in Physics at Karlsruhe Institute of Technology. Her Master thesis focuses on the coupling of photonic wire bonds to vertical device facets.

Tobias Hoose received his diploma in Physics at Karlsruhe Institute of Technology in 2012. During his diploma thesis he was working at the Institute of Photonics and Quantum Electronics (IPQ) on the topic of photonic wire bonds. In 2013 he started to work as doctoral candidate at the Institute of Microstructure Technology (IMT). His work is dealing with novel concepts and fabrication methods for multi-chip systems based on photonic wire bonds for future terabit/s transceiver modules.

Muhammad Rodlin Billah got his M.Sc. in Optics and Photonics from Karlsruhe Institute of Technology (KIT) and is currently working towards his PhD in the photonic wire bond group at KIT to build terabit/s DWDM transceiver systems. His work is supported by Helmholtz International Research School of Teratronics (HIRST)

Temitope Paul Onanuga received his B.Sc. degree in Engineering Physics from Obafemi Awolowo University, Nigeria in 2010. He is currently working towards the M.Sc. degree in Optics and Photonics at Karlsruhe Institute of Technology. His Master thesis focuses on advanced taper geometries for reduced losses in photonic wire bonds.

Andreas Hofmann received his Dipl.-Ing. in mechanical engineering from the University Karlsruhe (TH). He has worked in the field of automated production of e.g. micro systems more than 15 years. He is currently working in the field of micro assembly systems and processes at the Institute for Applied Computer Science (IAI) at Karlsruhe Institute of Technology. His main research interests lie in the field of comprehensive process and system design for micro manufacturing processes and the implementation in modular and adaptable system solutions.

Wolfgang Freude received the Dipl.-Ing. (M.S.E.E.) and the Dr.-Ing. (Ph.D.E.E.) degrees in Electrical Engineering in 1969 and 1975 from the University of Karlsruhe, Karlsruhe, Germany, respectively. He is currently a Professor at the Institute of Photonics and Quantum Electronics and a Distinguished Senior Fellow at Karlsruhe Institute of Technology. His research activities include the area of optical high-data rate transmission, high-density integrated-optics with a focus on silicon photonics, photonic crystals and semi-conductor optical amplifiers, and in the field of low-energy opto-electronic devices and protocols for optical access networks. He has published more than 250 papers, coauthored a book entitled "Optical Communications" (Berlin, Germany, Springer-Verlag, 1991, in German), and authored and co-authored four book chapters on "Multimode Fibres" in Handbook of Optical Communications (Berlin, Germany: Springer-Verlag, 2002, in German), "Microwave Modelling of Photonic Crystals" in Photonic Crystals—Advances in Design, Fabrication, and Characterization (Berlin, Germany: Wiley-VCH, 2004), "Linear Semiconductor Optical Amplifiers" in Fibre Optic Communication—Key Devices, Berlin, Germany: Springer-Verlag, 2012, and "Optical OFDM and Nyquist Multiplexing" in Optical Fiber Telecommunications VI B.

Systems and Networks (Amsterdam, Elsevier, 2013). Prof. Freude is an Honorary Doctor of the Kharkov National University of Radioelectronics, Kharkov, Ukraine, and a Member of VDE/ITG, and OSA. He serves in the Technical Program Committee "Photonic Networks and Devices" (OSA Advanced Photonics Congress 2013 and 2014), and was the Chair of the Subcommittee "Micro- and Nano-Photonic Devices" for CLEO 2012 and 2013. Until 2010, he was the Vice Chair of the IEEE Germany Photonics Society Chapter. From 2002 to 2006, he served as the Spokesman of the Research Training Group "Mixed Fields and Nonlinear Interactions," which was funded by the Deutsche Forschungsgemeinschaft (DFG) to support young researchers in their pursuit of a doctorate.

Christian Koos is a full professor at Karlsruhe Institute of Technology (KIT), where he is heading the Institute of Photonics and Quantum Electronics (IPQ) and the Institute of Microstructure Technology (IMT). His research focusses on integrated photonics and the associated applications in high-speed optical communications, biophotonics, as well as optical sensing and metrology. Christian Koos received the PhD (Dr.-Ing.) degree in Electrical Engineering from the University of Karlsruhe in 2007. From 2008 to 2010, he was affiliated with the Corporate Research and Technology department of Carl Zeiss AG, where he led the technology forecast in area of nanotechnology. In 2012, Christian Koos received the Alfried-Krupp Prize for Young University Teachers, one of the most highly endowed prizes for young researchers in the field of natural science and engineering at German universities. Christian Koos is the coordinator of the Helmholtz International Research School of Teratronics (HIRST), which offers an interdisciplinary training programme for PhD researchers that links the traditional disciplines of physics, electrical engineering, computer science, and nanotechnology.